

DETERMINING SURFACE TYPE FROM SURFACE NORMALS

Paul Amaranth  
Academic Computer Services  
Oakland University  
Rochester, MI  
48063

William Jaynes  
Intelligent Systems Laboratory  
Department of Computer Science  
Wayne State University  
Detroit, MI 48202

ABSTRACT

By exploiting the relationship which exists between the Gaussian image and gradient space, the two representations can be utilized in conjunction to facilitate the interpretation of a set of surface normals. The projection of the Gaussian image onto a plane can provide clear traces which quickly yield general knowledge of the underlying surface.

but only the binary image. This binary image is a discreet version of the space we term the Unit Gradient Space (UGS). Analysis using the UGS provides a promising technique for quickly acquiring basic information about the surfaces under consideration.

I Introduction

There are many methods in low-level machine vision which derive the 3-D surface orientation at each coordinate point in an image. Optical flow [1,8], texture gradient [7], and photometric stereo [2,6] are all techniques used to generate these surface normal vectors. Methods have been suggested for object recognition [5] and segmentation [3] using these normals. In general, however, the process of interpreting this local information to infer the underlying surface type is not well understood. This paper addresses the question: Given a collection of surface normals generated from a single, smooth surface, what can be determined about the surface? Using a variation of the gradient space, we present an approach for distinguishing simple surfaces. Our representation is purposely simple and limited as our object is to quickly obtain some basic knowledge of the surface.

III Image and Gaussian Space

The image model is entirely viewer centered. The observer looks along the Z axis with the Y axis pointing up and the X axis pointing to the right. The scene is orthogonally projected onto the image at Z=1.

With the image coordinate system defined, we now consider the coordinate system of the various gradient spaces. The UGS is closely related to gradient space and the gaussian sphere. If the equation for a smooth surface is of the form  $z=f(x,y)$ , then the observer directed normals to that surface are given by:

$$[p, q, -1] = [x/z, y/z, -1] \text{ eq. 1}$$

(Fig. 1) Gradient space consists of the points [p,q] each of which represents a particular surface orientation. The gaussian sphere is a sphere of unit radius. Each point on its surface represents the orientation of the plane tangent to the sphere at that point. The gaussian sphere can be defined as tangent to the gradient space at the gradient space origin. Kender [7] illustrates the relationships among the various spaces very clearly. If the gaussian sphere and

II Representation

If spatial information is ignored and all surface normals generated from an image are translated to a common origin, the gaussian image is formed [4,9]. This image can be seen as the locus of points formed by the intersection of the unit normals with a unit sphere called the Gaussian sphere. Any rotation in the scene causes a corresponding rotation of the Gaussian sphere about its origin. Histograming the X and Y components of the unit normals produces a 2-D approximation of the Gaussian image called the Gaussian histogram [3]. At the present time, we do not utilize the cell counts of the histogram,



Fig. 1. The observer directed normals of a conical and a cylindrical surface.

the gradient space are embedded within the scene coordinate system such that the following conditions hold:

- 1) The gradient space is defined by the plane  $Z=-1$
- 2) The  $p$  and  $q$  axes are aligned with and of the same units as the  $x$  and  $y$  axes
- 3) The center of the Gaussian sphere is at the origin

then a number of interesting properties become readily understandable. For the current discussion, however, the most important result is that the rotational coupling of the various spaces becomes obvious. Refer to figure 2. Gradient space then corresponds to a central projection of one hemisphere of the gaussian sphere onto the  $Z=-1$  plane. The UGS can clearly be seen as an orthogonal projection of the same hemisphere onto the  $Z=-1$  plane. Hence, it is a bounded version of gradient space and consists of the points

$$[p1, q1] = [p, q] / \|[p, q, -1]\| \quad \text{eq. 2}$$

#### IV Discussion

We are concerned with surfaces, not entire objects [5] and, at this point, we will narrow our perspective to encompass only single surfaces. As a further restriction, we will consider only conical and cylindrical surfaces with a circular cross section. We do this for two reasons. First, the form of their Gaussian images are straightforward and easy to visualize. Cylinders lie along arcs of great circles and cones form arcs on lesser circles. Secondly, they are singly curved surfaces and therefore representative of a class of surfaces

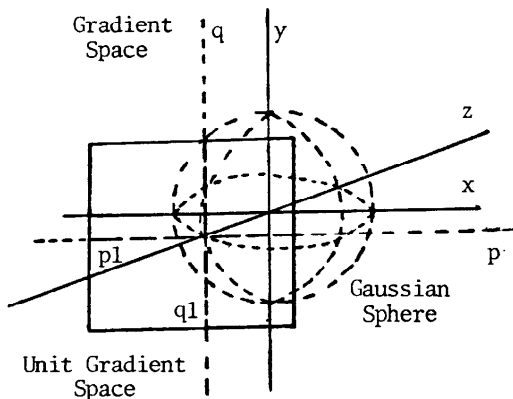


Fig. 2. The embedding of the Gaussian sphere, gradient space, and the unit gradient space into the scene coordinate system.

intermediate in complexity; falling between general and planar surfaces. In particular, any singly-curved surface must result in a one-parameter curve in gradient space [10] and, consequently, also in the UGS.

Given a curve in the UGS, we want to know if we can determine whether it indicates a cylinder or a cone and what, if any, parameters of the surface can be determined. First, let us assume that the axis of the cone or cylinder generating the surface is parallel to the image plane. Since a rotation about the  $Z$  axis results in a corresponding rotation in the UGS, we can assume without loss of generality that the axis is parallel to the  $Y$  axis. It can be shown that a right circular cylinder results in points on a curve in the UGS given parametrically by

$$p1 = \sin(t), q1 = 0 \quad \text{eq. 3, 4}$$

The curve in the UGS for a right circular cone is given by

$$p1 = b \cdot \sin(t) / (b^2 + 1),$$

$$q1 = 1 / (b^2 + 1) \quad \text{eq. 5, 6}$$

where  $b$  is the ratio of height to the radius of the base. These equations show that in the given orientation, conical and cylindrical surfaces give rise to straight line segments in the UGS. Intuitively, it is easy to see that the projection of an arc of a sphere onto a plane perpendicular to the plane defined by that arc will result in a line segment. The UGS line for a cylinder will pass through the origin, while that of the cone cannot. Further, the ratio of the height to the radius of the base of a cone is given by

$$b = 1 / (1 / q1^2) - 1 \quad \text{eq. 7}$$

In real scenes, it is unlikely that objects will be so conveniently oriented. As a consequence, the UGS representation of either a cone or a cylinder in some arbitrary orientation may describe a section of an ellipse. Consequently, the various surfaces are not distinguishable. Another possibility for standard orientation is suggested by the following observation. If a singly-curved surface is oriented such that a plane tangent to the surface is parallel to the image plane, the UGS curve of that surface will pass through the origin. The point on the curve at the origin corresponds to the ruling on the surface determined by the tangent plane. Conversely, if the UGS curve of a singly-curved surface passes through the origin, then there exists a ruling on the surface with a tangent plane which is parallel to the image plane. Thus, a standard orientation can be defined as one in which some ruling of the surface is parallel to the image plane. For a cylinder, this is equivalent to setting the axis of the surface parallel to the image plane and results in a straight line

through the origin of the UGS. The UGS curve for a cone will still lie on an ellipse, however. Thus we have a fast method of distinguishing the surfaces.

In this standard orientation, equation 7 will not necessarily be valid. It is still possible to recover the ratio of height to the radius of the base, however, by exploiting the fact that symmetries in a surface are reflected by symmetries in the Gaussian image. The center of the arc in the Gaussian image will correspond to a ruling down the center of the cylinder or cone. The following procedure is based on this observation.

### V Method

The method of standardizing the object position relative to the observer consists of two parts. The first part rotates the Gaussian image so that the center of the arc lies on the Z axis; that is, the center of the arc is at the origin of the UGS. This effectively rotates the surface so that the plane tangent to the approximate middle of the surface is parallel to the image plane. The second part performs a rotation about the Z axis so that the UGS curve is symmetrical with respect to the q1 axis. For

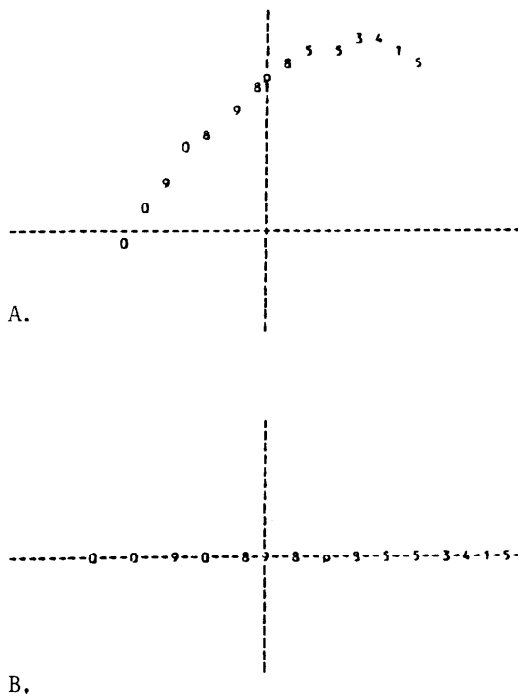


Fig. 3. Gaussian histograms for a cylinder in (a) an unstandardized position and (b) the standard position.

symmetrical surfaces, this has the effect of aligning the projection of the y axis of the surface with the q1 axis of the UGS.

At this point, conical and cylindrical surfaces are easily distinguished. It is also possible to recover the ratio of height to the radius of the base in the form of the angle at the apex of the cone. In this orientation, the distance between the endpoints of the curve in the UGS is a measure of the angle of the apex of the original conical solid. For a circular cone, this angle is equal to:

$$2 * \text{acos}(\text{dist} / 2) \quad \text{eq. 8}$$

This yields only an approximate value, however, because of the digitization problem mentioned later.

### VI Results

Data for analysis was generated by a program which, given the parameters of an object, produced the normals for the visible surface. The surface normals were produced by analytically determining the orientation of each of the surface patches as sampled through a 30 by 30 grid in the image space. A variety of cylindrical and conical surfaces at various orientations were manufactured. The resulting sets of normals were processed using the method described above. In all cases, the surfaces were brought either to, or very close to, a standard orientation. Figures 3 and 4 show typical

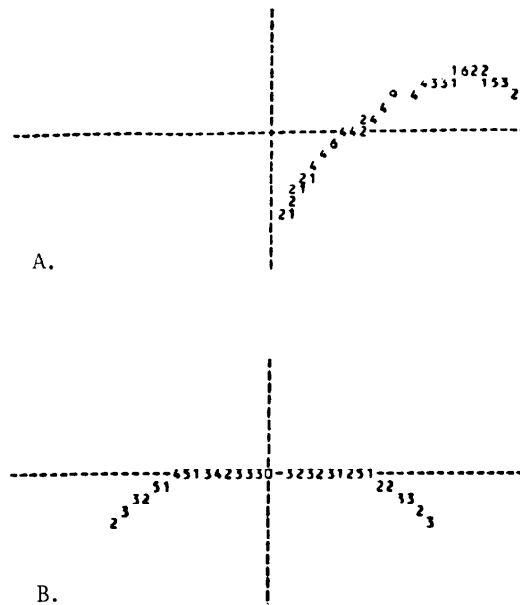


Fig. 4. Gaussian histograms for a cone in (a) an unstandardized position and (b) the standard position.

results for a circular cylinder and a circular cone. The differences between conical and cylindrical surfaces are readily apparent. For conical surfaces, equation 8 was used to determine the angle of the apex. Results are illustrated in table 1. As can be seen, the computed values are within thirteen percent of the actual values calculated analytically. Note the robustness of the method; consistent values are obtained regardless of the starting orientation of the surface.

Table 1.

Apex angles calculated for various circular cones at different orientations, using equation 8. All values in degrees.

| Actual Angle | Z Rotation | X Rotation | Computed Angle |
|--------------|------------|------------|----------------|
| 53           | 20         | 20         | 61             |
| 53           | 30         | 30         | 59             |
| 67           | 45         | 45         | 76             |
| 67           | -45        | -45        | 76             |
| 90           | 0          | 0          | 96             |
| 90           | 0          | 45         | 96             |
| 110          | 0          | 0          | 112            |
| 110          | -20        | -20        | 112            |
| 127          | 20         | 20         | 134            |
| 127          | 30         | 30         | 134            |

#### VII Concluding Remarks

The UGS image is formed by quantizing and histogramming the normals. As Dane and Bajcsy [3] have pointed out, a major problem lies in quantization effects. Resolution will determine whether a curve in the UGS is seen as a point, a smooth curve or as disjoint points. Dealing with one surface at a time, however, allows the possibility of adjusting resolution.

Our method makes use of the symmetrical nature of the surfaces apparent in the standard orientation. Depending on the initial orientation of the surface, however, it may appear somewhat asymmetrical, resulting in a final orientation that is not quite equivalent to the standard defined above. A variety of approaches were used to counter this difficulty, but it has not been completely eliminated. This does not appear to be a major problem as the difference between the ideal orientation and that obtained is only a few percent.

When dealing with singly-curved surfaces, it may not be necessary for the input to contain only one surface. Different types of surfaces or

similar surfaces at different orientations result in distinct traces. This fact could be used to aid in segmentation [3].

Finally, there is much more information which has yet to be exploited. Flatter surfaces yield a more condensed image in the UGS. The parameters of the elliptical curve in the UGS reflect on the curvature of the generating surface. The counts in the cells of the Gaussian histogram concern the relative size and/or rate of curvature of a surface. These are all matters for further investigation.

#### REFERENCES

- [1] Clocksin, W.F. "Determining the Orientation of Surfaces from Optical Flow." Proc. AISB/GI, Hamburg (1978), pp. 93-102.
- [2] Coleman, E.N. and Jain, R. "Obtaining 3-Dimensional Shape of Textured and Specular Surfaces Using Four Source Photometry." Computer Graphics and Image Processing 18 (1982), pp. 309-328.
- [3] Dane, C. and Bajcsy, R. "Three-Dimensional Segmentation Using The Gaussian Image and Spatial Information." Proc. PRIP-81 (1981).
- [4] Horn, B.K.P. "Sequins and Quills-representations for surface topography." A.I. Lab., M.I.T., A.I. Memo 536 (1979).
- [5] Ikeuchi, K. "Recognition of 3-D Objects using the Extended Gaussian Image." Proc. IJCAI-81 (1981), pp. 595-600.
- [6] Ikeuchi, K. "Determining Surface Orientations of Specular Surfaces by Using the Photometric Stereo Method." IEEE Trans. PAMI, 3 (1981), pp. 661-669.
- [7] Kender, J. "Shape from Texture." Dept. of Computer Science, Carnegie-Mellon University, CMU-CS-81-102 (1981).
- [8] Prazdny, K. "Egomotion and Relative Depth Map From Optical Flow." Biological Cybernetics, 36 (1981) pp. 87-102.
- [9] Smith, D.A. "Using Enhanced Spherical Images." A.I. Lab., M.I.T., A.I. Memo 530 (1979).
- [10] Woodham, R.J. "Reflectance Map Techniques for Analyzing Surface Defects in Metal Castings." A.I. Lab., M.I.T., AI-TR-457 (1978).